Measurements and two-dimensional computer simulations of the hygrothermal performance of a wood frame wall

Geving, S.; Karagiozis, A. N.; Salonvaara, M. H.

Publisher's version / Version de l'éditeur:

Journal of Thermal Insulation and Building Envelopes, 20, April, pp. 301-319, 1997-04-01

Measurements and two-dimensional computer simulations of the hygrothermal performance of a wood frame wall

NRCC-41079

Geving, S.; Karagiozis, A.N.; Salonvaara, M.

April 1997

A version of this document is published in / Une version de ce document se trouve dans:
Journal of Thermal Insulation and Building Envelopes, 20, April, pp. 301-319, April 01, 1997

Measurements and Two-Dimensional Computer Simulations of the Hygrothermal Performance of a Wood Frame Wall

STIG GEVING*
Department of Building and Construction Engineering
The Norwegian University of Science and Technology (NTNU)
Alfred Getz v 3, N-7034
Trondheim, Norway

ACHILLES KARAGIOZIS
National Research Council Canada
Institute for Research in Construction
Building Performance Laboratory
Montreal Road, Bldg. M-24
Ottawa, Ont. K1A 0R6, Canada

MIKAEL SALONVAARA
VTT Building Technology
Building Physics
P.O. Box 1804
FIN-02044 VTT, Finland

ABSTRACT: Knowledge of the expected long-term performance of building envelopes subjected to simultaneous heat and moisture transport is critical during the design stage. In the past thirty years researchers have concentrated their efforts in extensive laboratory experiments. These experiments have been expensive as well as time consuming to conduct due to the slow moisture transport phenomena. This paper critically investigates a set of experimental results generated from laboratory

*Author to whom correspondence should be addressed.

1065-2744/97/04 0301-19 $10.00/0

haust air side, or both. This is necessary to ensure that the ventilation air supplied, or induced, into a house will be adequately distributed through all rooms. Accordingly, builders, designers, and mechanical contractors must make adequate provision for ventilation air distribution ductwork in new house construction and large renovation activities where mechanical ventilation is necessary.

Although distribution is a significant consideration in the design and installation of ventilation systems, other important factors such as energy efficiency, occupant comfort, and ease of operation must also be considered.

A full report on this research project is available from the Canadian Housing Information Centre.

The Canadian Housing Information Centre
Canada Mortgage and Housing Corporation
700 Montreal Road
Ottawa, Ontario
K1A 0P7

Telephone: (613) 748-2367
FAX: (613) 748-2098

NOTE FROM THE EDITOR

The following technical note describes the same project from a research perspective. By placing these two notes next to each other we have provided the reader with a much broader perspective on this new and challenging area of building systems performance.

controlled measurements on a wood frame wall construction, by employing a state of the art hygrothermal model. The analysis was carried out using the LATENITE model, a three-dimensional heat and moisture transport program tailored specifically for building envelope investigations. For the present simulations this model was adapted for two-dimensional conditions and hourly hygrothermal performances were predicted for a laboratory instrumented wood frame wall section. The investigation showed three main advantages of combining measurements and simulations. By carrying out simulations early in the design stage of laboratory experiments the experimental design will probably yield better quantification of data, placement and types of sensors, and assessment of workmanship influences, etc. Measurements can calibrate, adapt, or check calculated results. Finally, simulations can be performed to explain and interpret experimental results. Marrying experiments and modeling allows researchers to generate effective hygrothermal performance guidelines.

KEY WORDS: wood frame wall, moisture transport, laboratory experiments, hygrothermal model.

INTRODUCTION

HYGROTHERMAL (COMBINED HEAT, air, and moisture) performance of building envelopes dictates to a large extent the durability and service life of the building envelope. Deterioration can occur in various forms, i.e., surface damage discolourization by efflorescence, ageing processes, chemical damages, moisture induced salt migration, structural cracking due to thermal and moisture gradients, corrosion of steel, and mould or bacteria growth.

An extensive amount of literature exits on laboratory testing of various building envelope systems such as Thue et al. [1]. Unfortunately, a limited amount of consistent information can be extracted for moisture control design guidelines. One reason is that to date a reliable measurement probe for moisture content is not widely available. Indeed in most experimentation, only few spot moisture content measurements are made and these are usually associated with rather high levels of uncertainty. Furthermore, in almost all experimental building envelope studies, modeling has not been used in the design of the experiments. This has resulted in improper positioning of moisture and temperature sensors and documentation of the workmanship defects or non-idealities.

Recently, hygrothermal models have been used in many interesting building envelope applications [2]. The hygrothermal performance of wood frame walls has been investigated by the use of simulations in several publications, but most of these have employed a one-dimensional approach. Tsongas et al. [3] analysed the moisture performance of different wood frame wall designs in different climate situations using a one-dimensional heat and moisture model. Hagentoft and Harderup [4] investigated the importance of a vapor retarder and air leakage of a wood frame wall with cellulose loose fill insulation, also employing a one-dimensional model. Only a few two-dimensional simulations of the heat-air and moisture behavior of wood frame structure exist such as [5] where the effect of exfiltration on the hygrothermal behavior was investigated.

In this project, a critical analysis is performed on a particular laboratory experiment of a wood frame construction wall, employing a state of the art hygrothermal model. The LATENITE three-dimensional model was employed to critically review the measured hygrothermal performance of the wood frame construction wall. The LATENITE research model allows treatment of the building envelope system with coupled heat and moisture transport via diffusion and natural and forced convective air transport, capillary, and gravity flow mechanisms. This model permits the "capturing" of the various systems and subsystems anomalies of the building envelope and can be employed in analysis of laboratory experimental hygrothermal results. In this paper, the moisture content, and temperature distributions at various locations in the wall were critically compared between laboratory measurement and two-dimensional computer simulations.

DESCRIPTION OF WALL EXPERIMENTS

This section gives a brief description of experiments conducted by Bigseth [6] to determine the hygrothermal performance of highly insulated wood frame walls. Tests were performed on six different wood frame walls in climatic chambers that were exposed to a sequence of winter conditions with cold external climate interrupted with short warm periods for a duration of sixty-eight days. In this investigation only one of the constructions was modeled. The wall system modeled was air- and vapor-tight on all boundaries, so any moisture movement within the wall assembly was due to internal redistribution only. This wall is not a typical construction, but is designed for laboratory experiments.

The wall section employed the following layers starting from the cold side: a 10 mm wood fiber board, a 0.15 mm PE-foil, 300 mm glass fiber batt insulation (density 18 kg/m^3), a 0.15 mm PE-foil, and a 9.5 mm gypsum board. Details of the construction are shown in Figure 1. The overall dimensions of the wall section were 1190 mm $\times$ 2390 mm, with stud and bottom/top plates dimensions of 36 mm $\times$ 300 mm (i.e., 98 mm + 198 mm). A PE-foil isolated the test wall perimeter from the surrounding constructions in terms of mass transfer (air and vapor), and adiabatic conditions at the wall perimeter with respect to heat transfer was present.

The locations of the measuring devices for moisture content and tempera-

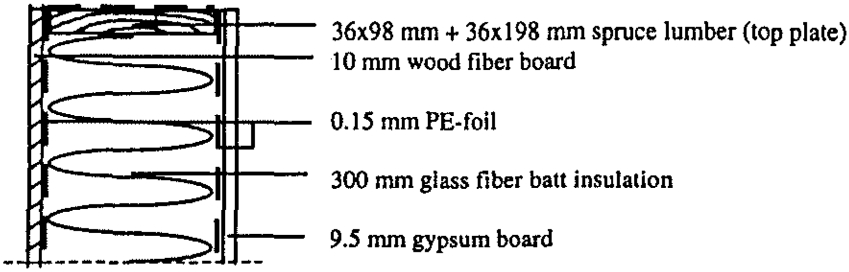

Figure 1. Top part of the wall section (wood fiber board on cold side).

ture are displayed in Figure 2. The moisture content of wood members was measured by the electric resistance method using a commercial moisture meter. The moisture meter used a calibration curve developed for Scandinavian spruce that considered different temperatures. The diameter of the metal electrodes used was 2 mm and they were covered with 0.5 mm plastic except for 1 cm at the tip. For the best possible adjustment between the elec-

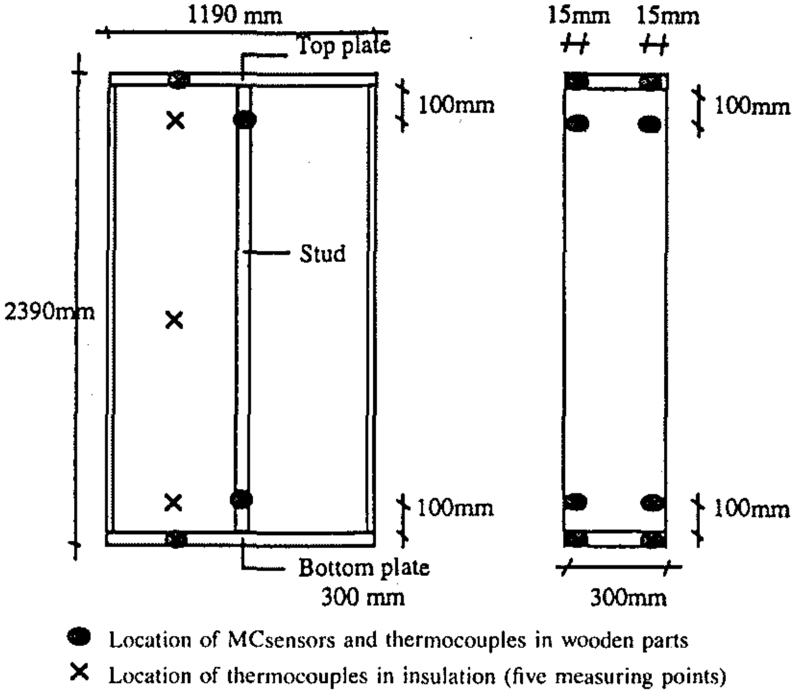

Figure 2. The framework of the wall test section, with measuring points.

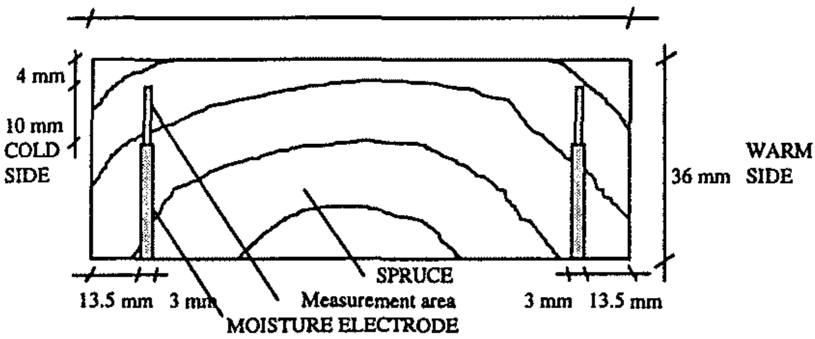

Figure 3. Detail of top plate showing location of moisture electrodes.

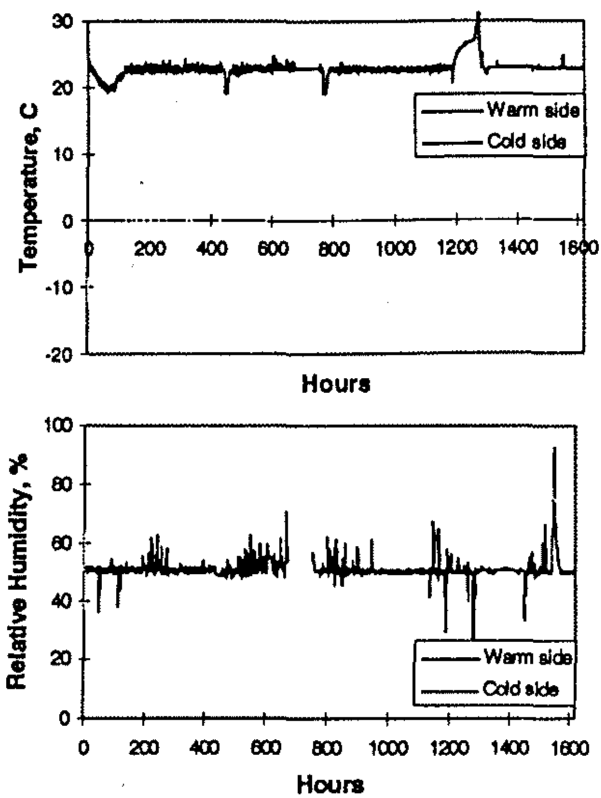

Figure 4. Air temperature and RH on warm and cold side of the construction.

Table 1. Vapor permeance of foil and board materials.

Material	Thickness [mm]	Vapor Permeance [kg/m² Pa·s]
Gypsum board	9.5	$2.5 \cdot 10^{-9}$
Wood fiber board	10	$3.63 \cdot 10^{-10}$
PE-foil	0.15	$3.11 \cdot 10^{-12}$

trodes and the material, the holes were drilled slightly smaller than the thickness of the electrodes. The top plate, the bottom plate, and the studs were instrumented for moisture and temperature measurements on the cold as well as the warm sides of the construction. The locations of the moisture electrodes in the top plate are shown in Figure 3. The temperature profile in the insulation was measured with rake of five thermocouples at the top, middle, and bottom section of the insulation layer. Measurements in the wood members were logged manually about every second day, while the temperatures in the insulation were logged automatically every hour.

The climate condition on the warm side was maintained at approximately 23°C and 50% relative humidity during the whole period. The cold side was kept constant for most of the time at about −15°C and between 70 and 90% RH. This cold climate was interrupted by two warmer periods of one week each in duration when the temperature was raised to approximately 3°C. In addition, there were short periods with temperature increases lasting only for a few hours due to defrosting requirements of the cooling equipment. The air temperature and relative humidity were logged hourly on both sides of the construction. The time dependent boundary conditions on warm and cold side are shown in Figure 4.

The vapor permeance of the foil and board materials was measured with the cup method (50%–94.1% RH), see Table 1.

DESCRIPTION OF MODEL

A detailed description of the LATENITE version 1.0 hygrothermal model is given by Karagiozis [7], Salonvaara and Karagiozis [8], and Hens [2], and only a brief overview is presented here with regard to the additional features imbedded in version 1.2. The moisture transport potentials used in the model are moisture content and vapor pressure; for energy transport, temperature is used.

The LATENITE 1.2 model has been recently upgraded to include porous air flow through insulation and cracks by solving a subset of the Navier Stokes equations: Darcy's equations. In addition, the solution domain has been extended to three-dimensions, allowing real practical problems to be solved. The model recently included the capability for handling internal heat and moisture sources, gravity driven liquid moisture, and surface drainage capabilities. The moisture transfer equation including liquid and vapor transfer is

$$\dot{m}_M = -\varrho_0 D_w(u,T)\nabla u - \delta_p(u,T)\nabla P_v + \nu_a \varrho_v + K(u)\varrho_w \vec{g}$$

where

$\dot{m}$ = mass flux, kg/m²·s
ϱ_0 = dry density of porous material, kg/m³
D_w = liquid moisture diffusivity, m²/s
u = moisture content, kg_w/kg_d
T = temperature, °C
δ_p = vapor permeability, kg/s·m·Pa
P_v = vapor pressure, Pa
ν_a = velocity of air, m/s
ϱ_v = density of vapor in the air, kg/m³
K = moisture permeability, s
ϱ_w = density of liquid water, kg/m³
g = acceleration due to gravity, m/s²

DESCRIPTION OF TWO-DIMENSIONAL CALCULATIONS

Several calculations were carried out to simulate the wall experimental system. The studs in the wood frame wall cannot be fully represented in two-dimensional modeling, but they do represent the most significant moisture capacity in the real structure. A case with high initial moisture content in the insulation was made to take into account the moisture capacity of the studs. The possible intrusion effect due to the presence of the electrode pins was also investigated. Mounted from inside of the cavity, these electrodes intrude through a rather wet area in the spruce and into a dryer region where the resistance is measured. Under these conditions, capillary transport of moisture along the electrodes into the dryer region could be present, thereby yielding corrupted moisture content readings. In a wood frame wall with low density batt insulation, nonperfect contacts could be present at material interfaces which will allow air leakage routes. These non-idealities can significantly alter the local effects of the internal air convection. To investigate these effects, some cases were modeled with air pockets (defects) at these material interfaces.

Boundary Conditions

A vertical cross section of the wall was modeled (300 mm × 2390 mm), including the top plate, bottom plate, and the insulation cavity. The PE-foil and the board materials were regarded only as resistance layers and included in the total surface resistances. The heat and moisture transfer surface resistances for the cold and warm side are shown in Table 2. The top and bottom boundaries were considered adiabatic assuming no heat and moisture transfer. The temperature and relative humidity at the warm and cold side were measured as shown in Figure 4.

Initial Conditions

The initial moisture contents were 0.14 kg/kg for the top plate, and about 0.135 kg/kg for the bottom plate. The average moisture content of the studs were about 0.14 kg/kg. This was measured by the electric resistance method right after the elements were built. The initial moisture content of the glass fiber was not measured, but judging from laboratory conditions, a relative humidity of about 65%, or approximately 0.0046 kg/kg was used.

Material Properties

The basic material properties that were used for spruce and glass fiber are given in Table 3. The sorption curve in the hygroscopic area for spruce was taken from measurements documented by Ahlgren [9] and adjusted to a temperature of approximately 5°C, not taking hysteresis into account. For the sorption curve above 98% RH, the moisture content-water potential relationship of aspen sapwood, was employed [11]. The vapor permeability-RH relationship of the spruce was taken from measurements documented in References [12] and [13]. The liquid diffusivity for spruce in the transversal

Table 2. Heat and moisture transfer resistances for cold and warm side surfaces.

Property	Cold Side	Warm Side
Thermal surface resistance, m^2 K/W	0.13	0.13
Thermal resistance fiber board, m^2 K/W	0.13	
Thermal resistance gypsum board, m^2 K/W		0.04
Total thermal surface resistance m^2 K/W	0.26	0.17
Total moisture surface resistance, $m^2 s$ Pa/kg	$3.2 \cdot 10^{11}$	$3.2 \cdot 10^{11}$

Table 3. Basic material properties for spruce and glass fiber (dry values).

Material	Density [kg/m³]	Specific Heat Capacity [J/kg K]	Thermal Conductivity [W/mK]	Vapor Permeability [kg/ms·Pa]	Air Permeability [m²]
Spruce	425	2390	0.08	$1.31 \cdot 10^{-12}$	$6.0 \cdot 10^{-14}$
Glass fiber	18	712	0.043	$1.43 \cdot 10^{-10}$	Horiz.: $2.5 \cdot 10^{-9}$ Vert. $5.0 \cdot 10^{-9}$

direction was estimated from measurements of the longitudinal liquid diffusivity-moisture content relationship and water absorption coefficients for longitudinal and transversal directions [10]. The sorption curves for the spruce and the glass fiber and vapor permeability and liquid diffusivity for the spruce are shown in Figure 5.

Investigated Cases

Five different cases were simulated, all cases being variations of the basic case as described previously. These cases are described in Table 4.

For Case 2, the initial moisture content in the glass fiber was augmented to 0.207 kg/kg. This represents all the initial moisture content in the studs uniformly distributed in the insulation. The possible effect of capillary transport along the moisture electrode was investigated in Case 3 by inserting a material layer with a very high liquid diffusivity and vapor permeability where the electrodes were located on the cold side. In Case 4, the effective air permeability of the glass fiber was increased to $1.0 \cdot 10^{-8}$ m² for both the x- and y-directions. In Case 5, the presence of air layers of thickness 10 mm at the interfaces top-plate/glass fiber, gypsum board/glass fiber, bottom plate/glass fiber, and fiber board/glass fiber was investigated.

Table 4. Description of the investigated cases.

Case	Description
1	Base case
2	Effect of high initial moisture content (MC) in insulation
3	Intrusion effect of MC electrodes
4	Effect of high air permeability of insulation
5	Effect of air gaps at material interfaces

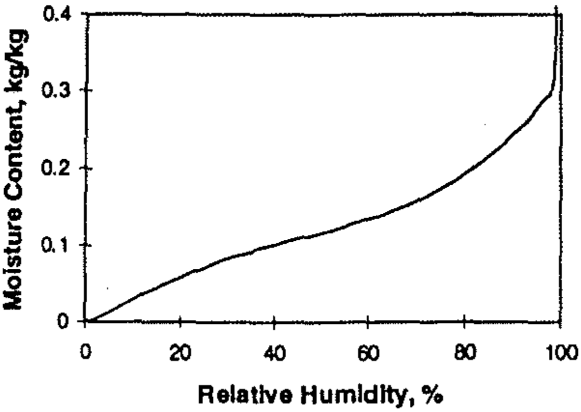

(a)

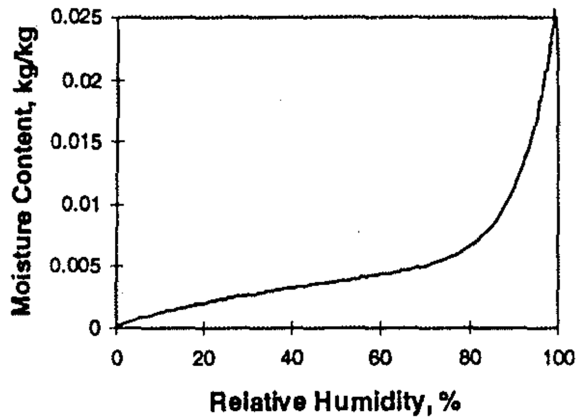

(b)

Figure 5. Sorption isotherm for spruce and glass fiber, and vapor permeability and liquid diffusivity for spruce. (a) Sorption isotherm for spruce, MC at capillary saturation is 1.8 kg/kg. (b) Sorption isotherm for glass fiber. Maximum MC at 100% RH is 50 kg/kg. (c) Vapor permeability for spruce. (d) Liquid diffusivity in transversal direction for spruce.

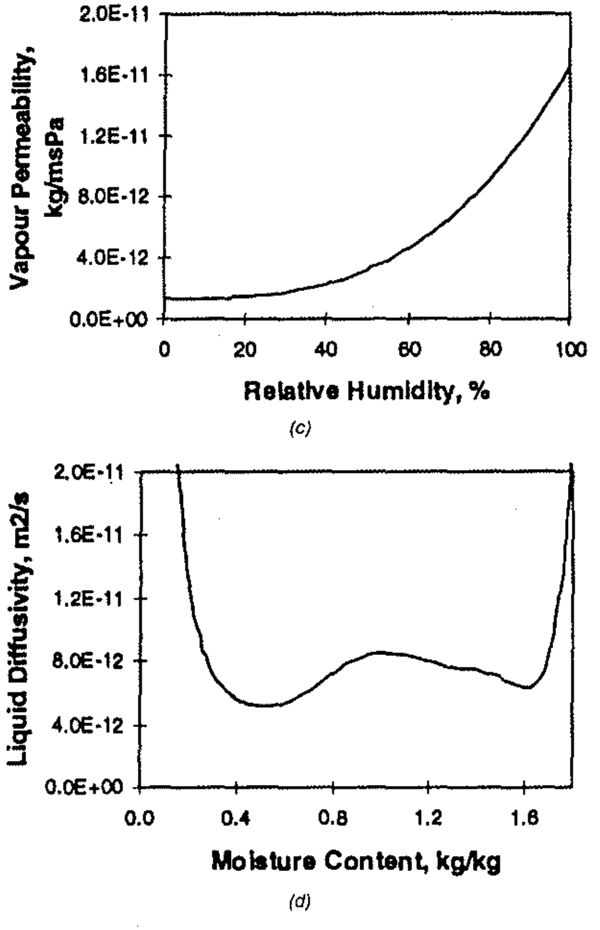

Figure 5 (continued). Sorption isotherm for spruce and glass fiber, and vapor permeability and liquid diffusivity for spruce. (a) Sorption isotherm for spruce, MC at capillary saturation is 1.8 kg/kg. (b) Sorption isotherm for glass fiber. Maximum MC at 100% RH is 50 kg/kg. (c) Vapor permeability for spruce. (d) Liquid diffusivity in transversal direction for spruce.

RESULTS AND DISCUSSION

The calculated moisture distribution within the insulation cavity for Case 1 is shown in Figure 6. With a low initial moisture content (MC) in the insulation, most of the moisture redistributes and condenses in the outermost part of the insulation within a few days. With a higher initial moisture content as in Case 2, this redistribution requires more time, but eventually most of the moisture has accumulated in the outermost nodal layer of the insulation. At this most exterior location, most of the moisture has accumulated in the top and bottom parts of the construction and less in the middle, with the highest MC at the top. The MC distribution in the top plate shows signs of drying on the warm side and wetting on the cold side (Figure 7).

The calculated moisture contents at the warm side of top and bottom plate show good agreement with the measured values for all the calculated cases, drying from MC of about 0.135 kg/kg to about 0.11 kg/kg (see Figure 8). This is not unexpected, since the warm part of the wood will be in the hygroscopic region during the calculation period. That means that the moisture transfer is mainly due to vapor diffusion, avoiding the possible problems that may be related to measuring and calculating wet wooden parts.

The agreement between measured and calculated MC on the cold side of the top and bottom plate is dependent on the selection of the measuring location. The tip of the moisture pins are located approximately 20 mm from the material interface between the wood and the insulation, and if this point is considered as the measuring point, the disagreement between measured and calculated values becomes large. For instance, the calculated increase in MC for this point during the whole period was about 2% by weight, while the measured values showed an increase of about 15% by weight. The measurements furthermore show a high and rapid increase in moisture content on the cold side when a warm period starts. In an ideal wood specimen this is not likely to happen, since moisture must be transported through several centimeters of wood to arrive at the measurement area of the moisture sensor. The moisture transfer occurs in the transversal/radial direction of the wood fibers, where the liquid diffusivity is very small. The main moisture transfer process into the wood specimen is due to vapor diffusion, which can hardly explain a MC increase of nearly 10% by weight over a period of a few days. An alternative explanation of the differences between measurements and calculations is possible due to disturbances caused by the pin electrodes at high local moisture concentration. An ice layer may form on the cold parts of the surface of the top and bottom plate during the cold period, while in warmer periods this ice could melt allowing free water on

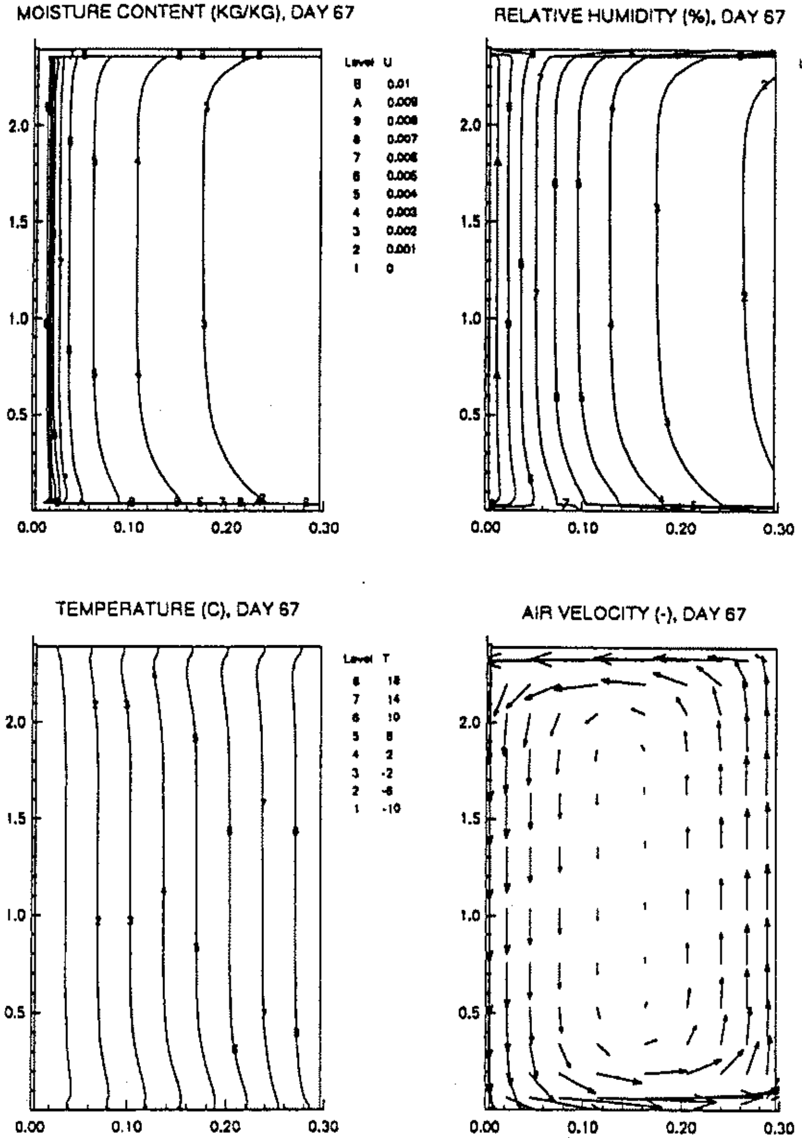

Figure 6. Case 1 – Base case. Calculated hygrothermal conditions within the wood frame wall at day sixty-seven.

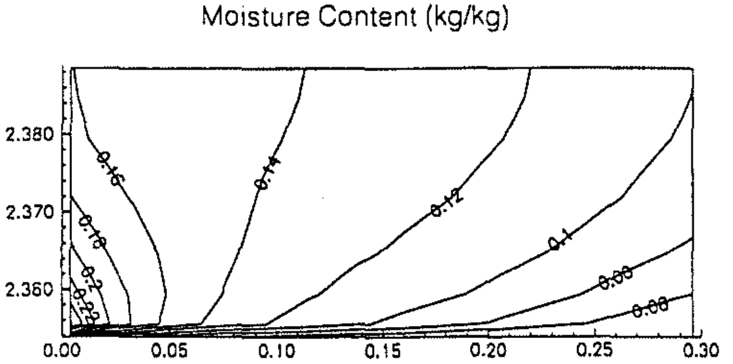

Figure 7. Case 1—Base case. Calculated moisture content in the top plate, day sixty-seven.

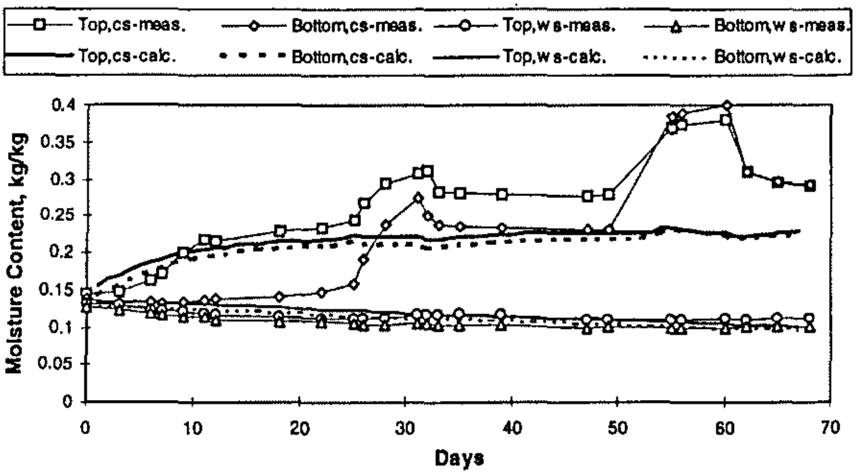

Figure 8. Case 1—Base case. Measured versus calculated values for moisture content in the top and bottom plate (cs = cold side, ws = warm side). The calculated values on the warm side are taken from the node that is located at the top of the electrode, while for the cold side the node that is located at the point where the electrode penetrate the spruce is used.

the wooden surfaces. Since the pin electrode intrudes through this wet area, it is possible that water is sucked into the pin opening at the interface between the electrode and wood causing high MC values.

The difference between calculated and measured moisture content at the bottom plate may also have other causes, one being dripping moisture against the PE-foil. Under freezing conditions a thin ice layer is formed on the PE-foil. As soon as the temperatures increase above 0°C this ice layer will melt, and water may run down the PE-foil and excessively moisten the bottom plate. The form of the measured curves (Figure 8), in fact, shows that a sudden moisture load appears at the bottom plate when the outside temperature passes through 0°C. At the same time, the sudden moisture load of the top plate cannot be explained through this hypothesis.

According to this conjecture, the measuring point on the cold side could actually be located at the wooden surface where the electrode pins intrude from the insulation cavity side. The agreement between measured and calculated values of MC for the cold side is good according to this hypothesis, as seen in Figure 8. The agreement is best for the top plate, while the bottom plate shows a higher MC at the beginning of the simulation. The calculated peak MC during the warm periods are not so distinct as the measured values.

The initial MC of the insulation has a significant effect on the calculated MC on the cold side of the top and bottom plates, demonstrated in Case 2 with about 2–5% by weight higher MC on the cold side than Case 1. The effect of the presence of the pin electrode was simulated in Case 3 by inserting a material with a very high liquid diffusivity and vapor permeability where the electrode was placed (see Figure 9). This gave an increase in MC at the tip of the electrode of about 1% by weight compared to Case 1. It can be seen that a major increase in moisture content appears during the warm periods. The effective air permeability of the insulation does not have a big effect on the calculated MC of the top and bottom plate. Though it should be noted that a higher air permeability yields a larger difference between MC at top and bottom plate, with the highest MC at the top plate.

Figure 10 shows measured versus calculated temperatures in the middle of the insulation at three different heights in the construction for Case 1. Agreement between measured and calculated temperatures is observed with respect to overall trend, however, point by point values deviate. The measurements indicate a higher degree of internal convection within the element than what is calculated for the ideal construction. It therefore seems reasonable to assume that non-idealities, such as air leakage paths at the interfaces of the material layers, occur in the construction. Figure 11 shows measured versus calculated temperatures for the case of air leakages at the material interfaces (Case 5). Only for the case with air leakage layers at all

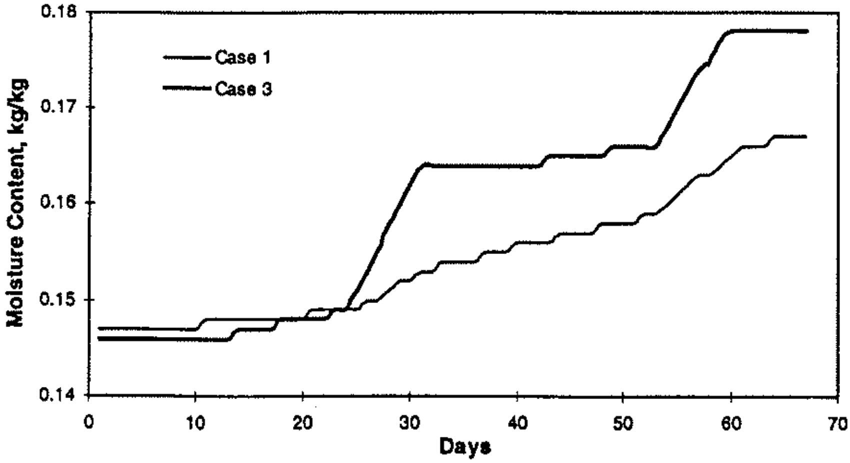

Figure 9. Case 3 – Modeling of intrusion effect of probe. Measured versus calculated values for moisture content in the cold side of top plate. The calculated values are taken from the node that is located at the top of the electrode.

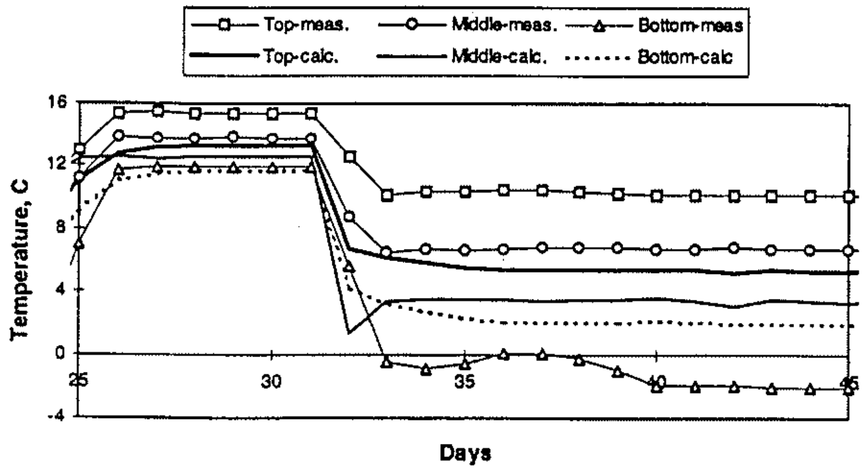

Figure 10. Case 1 – Basic Case. Measured versus calculated daily average temperatures in the middle of the insulation at three different heights in the construction. Day twenty-five to forty-five.

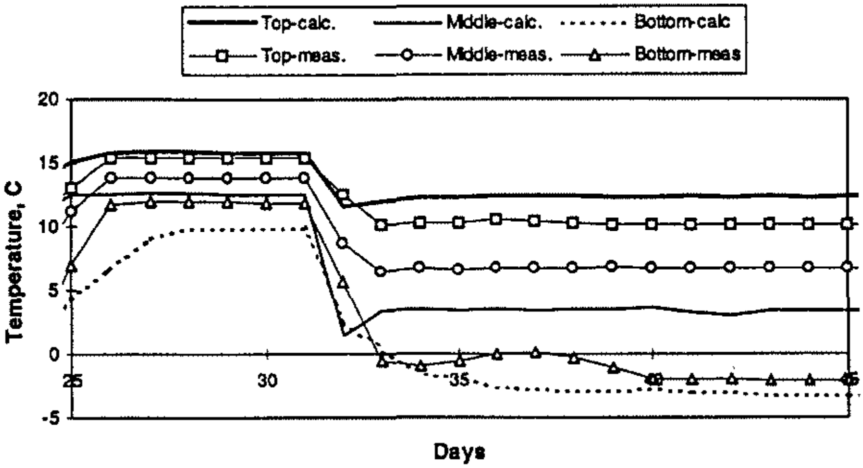

Figure 11. Case 5—Air layers at material interfaces. Measured versus calculated daily average temperatures in the middle of the insulation at three different heights in the construction. Day twenty-five to forty-five.

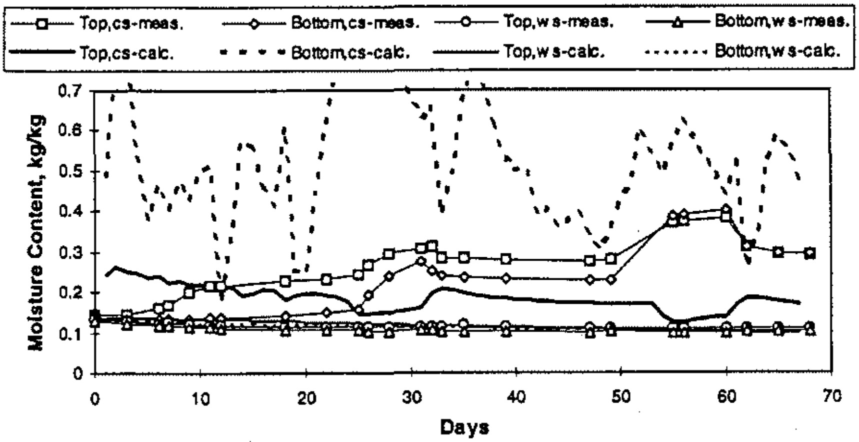

Figure 12. Case 5—Air layers at material interfaces. Measured versus calculated values for moisture content in the top and bottom plate (cs = cold side, ws = warm side). The calculated values on the warm side are taken from the node that is located at the tip of the electrode, while for the cold side the node that is located at the point where the electrode penetrate the spruce is used.

material interfaces, the calculated temperatures in the top and bottom parts show somewhat better agreement with the measured ones. Measurements show a higher temperature in the middle part of the construction than any of the calculated cases. This could be due to air leakage in the interface between the two insulation batts that are used in the cavity.

The calculated MC in the top and bottom plate for the cases with internal air leakage routes (Case 5) show good agreement with measured values for the warm side, see Figure 12. For the cold side there is no agreement when a vertical air leakage layer is included in the calculations. Though, it should be noted that when the construction was opened after the experiment was finished, it was observed that the bottom plate was very wet.

CONCLUSIONS

The measurements and model predictions of moisture content in the wooden parts show good agreement for the hygroscopic region. As soon as liquid water is present, the uncertainties associated with the measurement method make it difficult to compare measured and calculated values. When certain assumptions regarding the measurement method are made, the measured and calculated values show better agreement. Comparison of the measured and calculated temperature conditions indicate that the construction is highly affected by non-idealities in the cavity, indicating possibly a much higher degree of internal convection than for an ideal construction.

This study is an example that clearly shows that calculations should be made before designing laboratory experiments of this type. The most critical part of this experimentation is the location of the moisture electrodes. Preparatory calculations would have shown the importance of air gaps and where the highest moisture contents occurred. The electrodes placement could have been optimized using model predictions. It was quantitatively demonstrated that one should avoid positioning moisture electrodes through a wet part of the wood to measure at a dryer region.

Hygrothermal experimental investigations can be substantially enhanced at both the design phase and the analysis of the results by employing state-of-the-art models. As accurate moisture probes are not readily available, hygrothermal models that handle all the important moisture transport processes can be effective tools that can extract important moisture behaviours from critically reviewed experimental data.

The investigation showed the three main advantages of combining measurements and simulations, i.e.: (a) the use of preliminary simulation in the design, (b) the use of measurements to "calibrate," adapt, or check the calculated results, and (c) the use of modeling as a mean to explain and interpret the experimental results.

REFERENCES

1. Thue, J. V. et al. 1996. "Wood Frame Walls in Cold Climate—Vapour Barrier Requirements," *J. Thermal Insul. and Bldg. Envs.*, April.
2. Hens, H. 1996. "Final Report Task 1. Modelling Common Exercises. Summary Reports," International Energy Conservation in Buildings and Community Systems, *Annex 24 Heat, Air and Moisture Transport in New and Retrofitted Building Envelope Parts (HAMTIE)*.
3. Tsongas, G., D. Burch, C. Roos and M. Cunningham. "A Parametric Study of Wall Moisture Contents Using a Variable Indoor Relative Humidity Version of "MOIST" Transient Heat and Moisture Model," *Proceedings of the Sixth Thermal Performance of the Exterior Envelopes of Building Conference*, Dec. 4–8, Clearwater, Florida, pp. 307–319.
4. Hagentoft, C. E. and E. Harderup. 1996. "Moisture Conditions in a North Facing Wall with Cellulose Loose Fill Insulation: Construction With and Without Vapor Retarder and Air Leakage," *J. Thermal Insul. and Bldg. Evns.*, 19:228–243.
5. Ojanen, T. and K. Kumaran. 1996. "Effect of Exfiltration on the Hygrothermal Behaviour of a Residential Wall Assembly," *J. Thermal Insul. and Bldg. Envs.*, 19:215–227.
6. Bigseth, L. 1994. "Moisture and Temperature Conditions in Highly Insulated Building Constructions (in Norwegian)." M.Sc. thesis, Norwegian Institute of Technology, Dept. of Building and Construction Engineering, Trondheim, Norway.
7. Karagiozis, A. 1993. "Overview of the 2-D Hygrothermal Heat-Moisture Transport Model LATENITE," Internal Report, National Research Council Canada, Institute for Research in Construction, Ottawa, Canada.
8. Salonvaara, M. and A. Karagiozis. 1994. "Moisture Transport in Building Envelopes Using an Approximate Factorization Solution Method." CFD Society of Canada, Toronto, Canada.
9. Ahlgren, L. 1972. "Moisture Fixation in Porous Building Materials," Report 36, Div. of Building Technology. Lund Institute of Technology, Sweden.
10. Kumaran, M. K. 1996. "Material Properties, Final Report Task 3," International Energy Agency, Energy Conservation in Buildings and Community Systems, Annex 24 Heat, Air and Moisture Transport in New and Retrofitted Building Envelope Parts (HAMTIE). Laboratorium Bouwfysica, K.U.-Leuven. Belgium.
11. Cloutier, A. and Y. Fortin. 1991. "Moisture Content-Water Potential Relationship of Wood from Saturated to Dry Conditions." *Wood Science and Technology*, 25:263–280.
12. Tveit. A. 1966. "Measurements of Moisture Sorption and Moisture Permeability of Porous Materials," Norwegian Building Research Institute, Oslo, Norway.
13. Time, B. 1995. "Water Vapour Permeability Measurements of Spruce, Cup Measurements," Work Report No. 4, Norwegian Institute of Technology, Dept. of Building and Construction Engineering, Trondheim, Norway.